Matching Topographic Surfaces: Application to lidar and photogrammetric surfaces.

Frédéric Bretar [a,b], Michel Roux [b], Marc Pierrot-Deseilligny [a]
[a] Institut Géographique National
2-4 Av. Pasteur 94165 St. Mandé cedex, France
Email: {Frederic.Bretar, Marc.Pierrot-Deseilligny}@ign.fr
[b] GET-Télécom Paris - UMR 5141 - Département TSI
46 Rue Barrault 75013 Paris, France
Email: Michel.Roux@enst.fr

KEY WORDS: Lidar , 3D registration , robust estimation , matching ,data fusion ,DSM

ABSTRACT:

If photogrammetry has been used for a long time to describe the topography, airborne laser systems are nowadays well-known to provide an accurate representation of terrestrial landscapes through irregular 3D point clouds. Both technologies have their pros and cons that a joint use may optimize to reach a better description of 3D scenes. Beyond the adjustment problem of laser strips, combining optical and laser data is at first a registration problem, especially when using high resolution images. We propose in this paper a methodology for registering laser strips with regard to a photogrammetric derived Digital Surface Model (DSM) which has been computed from a set of known pose calibrated images. Based on the main hypothesis that the geometrical frames of laser systems and digital cameras are linked with a regular function, we describe an algorithm based on the calculation of linear approximations of this transform with 3D local translations. Due to the irregular spatial distribution of laser data and the difficulty of detecting homologous points in the DSM, we adopt a statistical strategy to find patch correspondences which leads to analyze the distribution of a certain vector set of potential homologous candidates. We then propose to estimate an analytical model through a weighted sliding window strategy. Laser strips are corrected globally in a chronological order. The algorithm is validated onto synthetic transforms. Experimental results show the capability of the registration algorithm on raw laser data sets.

1 INTRODUCTION

Airborne laser altimetry has been the first autonomous acquisition system providing fully georeferenced 3D data as point clouds. Supporting vector attitudes are optimally calculated using the synergy of both GPS and inertial measurements (Kilian et al., 1996) providing at the top end process an altimetric accuracy of less than $0.05\ m$ and a planimetric accuracy of about $0.50\ m$ or less depending on the flying conditions as well as on the surveyed topography (tridimensional structure). The knowledge of the error general behavior has been studied in details so far by many authors (Schenk, 2001) or manufacturers (Katzenbeisser, 2003). Among the general error budget, some of them can be calibrated (encoding errors, bias on the rotating mirror mechanics for concerned systems ...) whereas others cannot. It is well known that the later can be considered as consequences of the INS temporal drift. Nevertheless, the combination of the different error sources can be finally of such a form but a linear temporal drift (Ronnholm, 2004). The effects of orientation errors onto the final point clouds are sometimes particularly visible since a laser survey is acquired by strips of 100 m to 500 m width. It is the famous strip adjustment problem that has been partly sorted out by searching homologous plane surfaces lying onto the overlapping areas (Kager, 2004). If the relative coherence of a set of laser strips can be achieved, even if it is by manual processes, absolute accuracy of laser surveys over large areas is still a questioning topic. It is an essential point when it comes to use jointly laser data with other georeferenced data sources that are meant to be expressed with a certain absolute accuracy. Lidar data are no doubt a valuable source of altimetric information for photogrammetric campaign providing directly the altitude of a pixel with a better accuracy than using a correlation process (the better ones need to deal with multi-images). Nevertheless, it has been widely noticed that 3D offsets generally appear between laser points and their counter parts in the photogrammetric geometry (projection). This problem can be tackle either by searching for invariant features in the point cloud and in the oriented image before adjusting the image orientation (Habib et al., 2005), or directly working on the 3D data derived from the correlation processes and the lidar surface. One of the major difficulty is to deal with the relative dissemblance of both surfaces to match, seeing that they have no been acquired at the same time and above all, both technologies do not represent the same landscape with the same aspect. We can mention for instants that discontinuities over facades in an urban context are much sharper in the lidar data than in a photogrammetric Digital Surface Models (DSM). This part of the algorithm is validated onto simulated data.

We propose to develop in this study a full registration methodology for matching topographic surfaces acquired with different sensors, especially lidar point clouds and photogrammetric DSM. As an alternative to other registration methodologies based on the detection of characteristic features such as planes, we propose to match lidar surface patches with regard to the photogrammetric DSM. The algorithm is based on the local study of a distribution in the 3D translation space. We show that the maximum of this distribution is locally associated to the most probable local translation that makes both surface patches homologous

After detecting homologous surface patches (a non continuous 3D deformation field is derived for each laser strip), and alternatively to polynomial models with a potential temporal dependency, we apply an original correction technique based on the estimation of a transformation (affinity) through a sliding window. The final corrected point is a weighted mean of the independently processed correction calculated over successive sliding windows. The entire methodology has been validated onto simulated transforms with conclusive results. It has been applied onto real laser data showing a real, non linear 3D behaviour of the registration function.

2 THEORY

Let us consider two subsets of $\mathbb{R}^3$, $\mathcal{S}_{laser}$ and the DSM, representing both of them the same topographic landscape, but expressed into two different frames. Registering $\mathcal{S}_{laser}$ and the DSM consists in retrieving the unknown n parameter transform $\mathcal{M}_{th}$ that maps one geometry into the other. The registration problem is dual in case of a global deformation: First finding correspondences (tying features) followed by the estimation of a global transform $\mathcal{M}$ (a model of $\mathcal{M}_{th}$) minimizing a cost function

$$\mathcal{F}(\mathcal{M}) = \sum_i d(\mathcal{M}(X_i), Y_i) \quad (1)$$

where $X_i \in \mathcal{S}_{laser}$ and $Y_i \in$ DSM are the i^{th} homologous feature, d is a distance function. Tying features may be of different nature. As mentioned in the introducing part, point correspondences between lidar and DSM are difficult to calculate. We will therefore search for surface patch correspondences without any limitation on plane or linear feature extraction. We will search for correspondences by regularly paving laser strips.

2.1 Determination of patch correspondences

Considering the registration problem of a laser strip with regard to a DSM, we will suppose that $\mathcal{M}_{th}$ is regular enough to be approximated with piecewise shifts which represent the local offset between both point clouds. The calculation of these local shifts provides homologous patches of points which can be represented as homologous centroïds for convenience during the global estimation process.

Let us consider adjacent square regions R that pave a laser strip, and the set L_R of laser points included in R.

$$R = [x_1, x_2] \times [y_1, y_2] \in \mathbb{R}^2$$
$$L_R = \{l_k = (x_k, y_k, z_k)_{k\in[0,K]} \in \mathcal{S}_{laser} / \quad (x_k, y_k) \in R\}$$

$\mathcal{V}_{l_k}$ (equation 2) is a neighborhood of DSM points centered onto the planimetric coordinates of a laser point l_k. Note that the neighborhood's shape does not have any influence on the processing.

$$\begin{aligned}\mathcal{V}_{l_k} =& \{p_j = (x_j, y_j, z_j)_{j\in\mathbb{N}} \in \text{DSM} / \\ & max(|x_k - x_j|, |y_k - y_j|) \leq C\}\end{aligned} \quad (2)$$

where C is a constant.

Let $\overrightarrow{\widetilde{T}_{L_R}}$ be the *unknown* approximation of $\mathcal{M}_{th}$ (local shift) onto a surface patch L_R that we want to retrieve. Each point $l_k \in L_R$ will have a *nearest homologous point* (n.h.p) in $\mathcal{V}_{l_k}$ (provided that $\mathcal{V}_{l_k}$ be wide enough) through a translation $\overrightarrow{t_k}$ ($\overrightarrow{t_k}$ is reached when $\overrightarrow{p_j l_k}$ has the nearest orientation of $\overrightarrow{\widetilde{T}_{L_R}}$) satisfying:

$$\overrightarrow{t_k} = \arg\min \|\overrightarrow{p_j l_k} \wedge \overrightarrow{\widetilde{T}_{L_R}}\| \quad \forall l_k \in L_R,\, p_j \in \mathcal{V}_{l_k} \quad (3)$$

where $\wedge$ denotes the vector product of both vectors, $\overrightarrow{p_j l_k}$ (a potential shift candidate) is the vector between the extracted DSM nodes $\mathcal{V}_{l_k}$ and the laser point l_k, $\overrightarrow{t_k}$ and $\overrightarrow{\widetilde{T}_{L_R}}$ are unknown.

Since $\overrightarrow{\widetilde{T}_{L_R}}$ is supposed to be unique over the surface patch L_R, $\overrightarrow{\widetilde{T}_{L_R}}$ is the translation for which vectors $\overrightarrow{t_k}$ are similar for all laser points l_k in L_R. Equation 3 cannot be solved directly. Each point belonging to $\mathcal{V}_{l_k}$ is a potential n.h.p of l_k. The most represented potential n.h.p. may be seen as the maximum of the distribution $d_{\mathcal{P}}$ of $\mathcal{P} = \{\overrightarrow{p_j l_k}\}_{\forall l_k \in L_R,\, \forall p_j \in \mathcal{V}_{l_k}}$. $\overrightarrow{\widetilde{T}_{L_R}}$ is therefore defined as:

$$\overrightarrow{\widetilde{T}_{L_R}} = \arg\max_{\overrightarrow{X}\in\mathcal{P}} d_{\mathcal{P}}(\overrightarrow{X})$$

2.2 Estimation process

The point matching part of the algorithm provides piecewise shift approximations of $\mathcal{M}_{th}$. In order to estimate its analytical representation, we will consider both the initial point cloud and the piecewise corrected one by the above calculated $\overrightarrow{\widetilde{T}_{L_R}}$. The idea is to apply a continuous transform to the whole strip so that the final point cloud should be continuously corrected. We applied a 12 parameter affinity $(\mathcal{A}|\mathcal{T}_a)$ where $\mathcal{A}$ is any 3×3 matrix and $\mathcal{T}_a$ a 3D translation. $(\mathcal{A}|\mathcal{T}_a)$ is estimated using a least power estimation process. This estimator belongs to the family of robust M-estimators. Unlike the standard least-square method that tries to minimize $\sum_i r_i^2$ where r_i is the difference between the i^{th} observation d_i and its fitted value $H_{\mathcal{A}/\mathcal{R}} m_i$, the M-estimators try to reduce the effect of outliers by replacing the squared residuals r_i^2 by another function of the residuals yielding to minimize $\sum_i \rho(r_i)$ where ρ is a symmetric, positive function with a unique maximum at zero, and is chosen to be less increasing than square. Following Xu and Zhang (Xu and Zhang, 1996), for regression problems, the best choice is the L_p function which consists of minimizing

$$\sum_i \frac{\|d_i - H_{\mathcal{A}/\mathcal{R}} m_i\|^p}{p}$$

with $p = 1.2$. This optimization is implemented as an iterative re-weighted least power algorithm. In a robust cost model, nothing special needs to be done with outliers. They are just normal measurements that happen to be down-weighted owing to their large deviation.

2.3 Global Correction

The hypothetical time dependency is modelled with the estimation of a set of transforms (here, affinities) along the flight track through a sliding window of constant width w (strip width) and of tunable length L (see figure 1). L is defined to be linearly proportional to w ($L = aw,\ a \in \mathbb{R}^{+*}$). This window evolves with a defined moving step $k > 0$. We prefer to define an overlapping ratio $\zeta = 1 - \frac{k}{L}$ with $\zeta \geq 0.5$ so that a majority of laser point should be processed at least twice. Depending on k, a laser point will be processed $E[\frac{L}{k}]$ times where E is the integer part function. The final corrected point ($\overline{\bigotimes_{E[\frac{L}{k}]} M}$) will be their weighted mean value, which is motivated by the almost zero standard deviation of the independently processed 3D points. The weighting function $\mathcal{W}$ is defined as a Gaussian function depending on both ζ and on the distance $d \in [0, \frac{L}{2}]$ between the laser point M and a line defined by a normal vector of the flight track direction and the barycenter of the sliding window. We have

$$\mathcal{W}(d) = e^{-(\frac{d}{k})^2} = e^{-(\frac{d}{L(1-\zeta)})^2}$$

3 THEORETICAL EXPERIMENTS

3.1 Description

Before applying the algorithm onto raw laser data, several simulations have been performed. This simulation aims to decide whether or not the algorithm is able to retrieve a global motion through the detection of local 3D offsets as well as to evaluate its

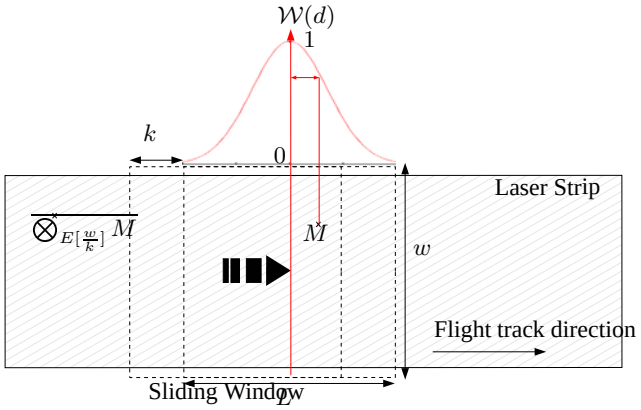

Figure 1: Sketch of the sliding window strategy with a $w \times L$ window (dotted rectangles). M is a laser point to be processed $E[\frac{w}{k}]$ times. $\overline{\bigotimes_{E[\frac{w}{k}]} M}$ is the mean of processed point M weighted by $\mathcal{W}(d)$.

ability of correcting a point cloud with regard to an other without applying the exact inverse transform, but approximation. In this respect, we need a simple deformation simulator that can simulate geometrical disturbances of a strip-like point cloud. In this section, we will consider the 3D point cloud as a set $\mathcal{E}_1$ of randomly under-sampled 3D points belonging to the DSM of final density $\sim 10\ pts/m^2$. The strip width (resp. length) equivalent is $\sim 240\,m$ (resp. $\sim 2250\,m$). $\mathcal{E}_1$ is modified into $\mathcal{E}_2$ through a theoretical isometry $(\mathcal{R}_{\omega(t),\,\phi(t),\,\kappa(t)}|\mathcal{T}(t))$ where angles $\omega(t)$, $\phi(t)$, $\kappa(t)$ and translation $\mathcal{T}$ are time-dependent. $\mathcal{E}_2$ is then registered with regard to the DSM defined previously. Note that in this simulation, all 3D points of $\mathcal{E}_1$ have an homologous point in the DSM.

The simulation consists in applying the transform $(\mathcal{R}_{\omega(t),\,\phi(t),\,\kappa(t)}|\mathcal{T}(t))$ onto $\mathcal{E}_1$ where the rotation center lies approximately on the ground. The flight track is in the middle of the strip. The planimetric coordinates of the rotation center are calculated for each 3D point of $\mathcal{E}_1$ along the flight track. Two examples of simulated transform are given hereafter. The first simulation (equation 4) describes the rotating angle evolution as a linear function of time. The second simulation (equation 5) describes the time dependency as a sinusoidal evolution. In equations 4 and 5, t_0 is the initial time, Δt is the flight duration and ω, ϕ, κ are respectively the yaw, pitch and roll rotating angle.

$$\begin{aligned} \omega(t) &= \tfrac{\omega_{\Delta t}-\omega_{t_0}}{\Delta t}t + \omega_{t_0} \\ \phi(t) &= \tfrac{\phi_{\Delta t}-\phi_{t_0}}{\Delta t}t + \phi_{t_0} \\ \kappa(t) &= \tfrac{\kappa_{\Delta t}-\kappa_{t_0}}{\Delta t}t + \kappa_{t_0} \end{aligned} \tag{4}$$

$$\begin{aligned} \omega(t) &= \omega_{t_0}\cos(2\pi\tfrac{t-t_0}{\Delta t}) \\ \phi(t) &= \phi_{t_0}\cos(2\pi\tfrac{t-t_0}{\Delta t}) \\ \kappa(t) &= \kappa_{t_0}\cos(2\pi\tfrac{t-t_0}{\Delta t}) \end{aligned} \tag{5}$$

3.2 Results

We compared three configurations for the global registration: our algorithm has been tested with the estimation of a set of affinities. Here, homologous patches are squares of $5m \times 5m$ containing roughly 250 3D points. A local shift is estimated every 5 meters in x and y. The DSM resolution is $0.24\ m$ and the z sampling rate of $d_{\mathcal{P}}$ is set to $0.05\ m$. Finally, we have applied a Rigid Transform with Time Dependency (*RTTD* in the following) (Kilian et al., 1996) (considering small angles, this transform can be written as equation 6) onto homologous patches. Initial values are set as follow:

$$\omega_{t_0} = 0.15^o,\ \omega_{\Delta t} = -0.15^o,\ \phi_{t_0} = 0.01^o$$
$$\phi_{\Delta t} = -0.01^o,\ \kappa_{t_0} = -0.03^o,\ \kappa_{\Delta t} = 0.03^o$$

$$\begin{pmatrix} x_1 \\ y_1 \\ z_1 \end{pmatrix} = \begin{pmatrix} \Delta X \\ \Delta Y \\ \Delta Z \end{pmatrix} + \begin{pmatrix} \delta X \\ \delta Y \\ \delta Z \end{pmatrix} t + \left[\begin{pmatrix} 1 & -\kappa & -\phi \\ \kappa & 1 & -\omega \\ -\phi & \omega & 1 \end{pmatrix} + \begin{pmatrix} 0 & -\dot{\kappa} & -\dot{\phi} \\ \dot{\kappa} & 0 & -\dot{\omega} \\ -\dot{\phi} & \dot{\omega} & 0 \end{pmatrix} t \right] \begin{pmatrix} x_2 \\ y_2 \\ z_2 \end{pmatrix} \tag{6}$$

where $(x_1, y_1, z_1)^T$ and $(x_2, y_2, z_2)^T$ are 3D homologous points.

Figure 2 represents a central profile of the theoretical and the retrieved deformations along the simulated flight track (**simulation 1**). Here, (D_x, D_y) (resp. D_z) are respectively the deformations in planimetry and in altimetry. The time dependency is linear in that case. One observes that the *RTTD* model is a good approximation of the linear deformation. Same results are obtained using the methodology developped in this paper.

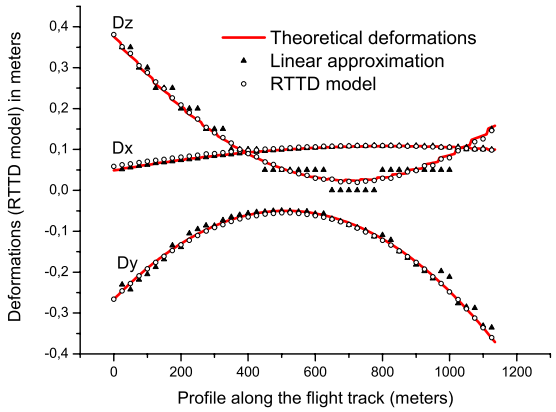

Figure 2: Comparison of the RTTD retrieved deformations with regard to **simulation 1**.

As far as **simulation 2** is concerned, we can notice that strong non linearities are globally retrieved using the sliding window strategy (figure 3, central profile along the flight track) whereas they are not using the *RTTD* model. Indeed, variations of theoretical deformations along the profile presented in figure 4 are generalized when estimating a linear time dependency.

Finally, it appears that correcting a laser strip using the sliding window strategy whereon affinities are successively estimated is an efficient methodology for modelling non linearities along the strip. It is of particular interest since errors observed along the strip may be of different natures, leading at the top end process to a 3D structure of the final strip deformation field (Ronnholm, 2004).

4 Experimental results and Discussion

The algorithm is designed to be independent of the laser system. It has been tested with raw laser data acquired over the city of

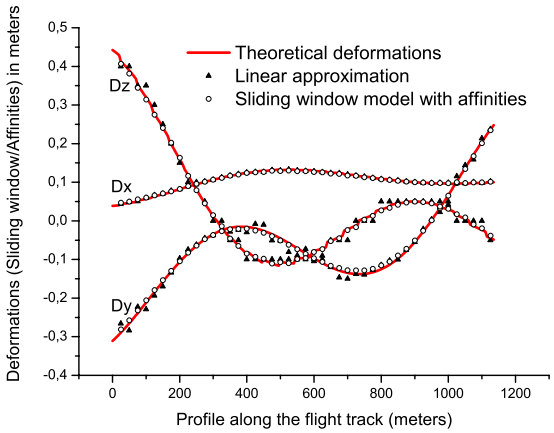

Figure 3: Comparison of the sliding window retrieved deformations with regard to **simulation 2**.

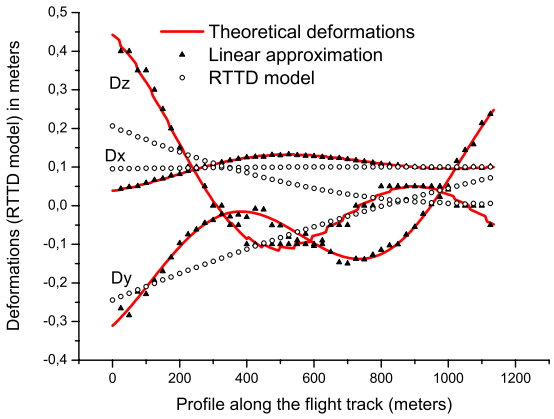

Figure 4: Comparison of the RTTD retrieved deformations with regard to **simulation 2**.

Amiens, France, by the company TopoSysⓒ. The spatial density of the data set is roughly one point every $0.1\ m$ along the flight track and one point every $1.2\ m$ in the cross-track direction. It is an average of $7.5\ points/m^2$ per strip.

The DSM is computed from correlation techniques using dynamic programing (Baillard and Dissard, 2000) along epipolar lines. The final reliable DSM with $0.2\,m$-resolution results from the fusion of a set of DSMs calculated from some pairs of aerial images. The theoretical altimetric accuracy of the DSM is $0.5\,m$ ($\frac{B}{H} = 0.4$) which is not as accurate as laser points' one.

Figure 5(a) represents the local surface matching onto raw laser data as well as the related modelled deformation field (figure 5(b). The correctness of the retrieved transform can be validated observing the different profiles in figure 6.

The tridimensional deformation pattern calculated by the presented methodology describing the function to be applied to a laser strip to be registered with regard to a photogrammetric surface does not represent the effective function which would lead to a better absolute accuracy of the laser survey. The aim of this method is to provide mutually referenced altimetric data in order to optimize the joint use of laser and photogrammetric data. Nevertheless, since the absolute planimetric accuracy of a photogrammetric DSM depends on the quality of the control points introduced in the aerotriangulation process, and seeing that it is easier to identify control points onto images, and therefore onto the DSM, we could expect to improve the absolute planimetric accuracy of laser data provided that the absolute accuracy of the DSM be better.

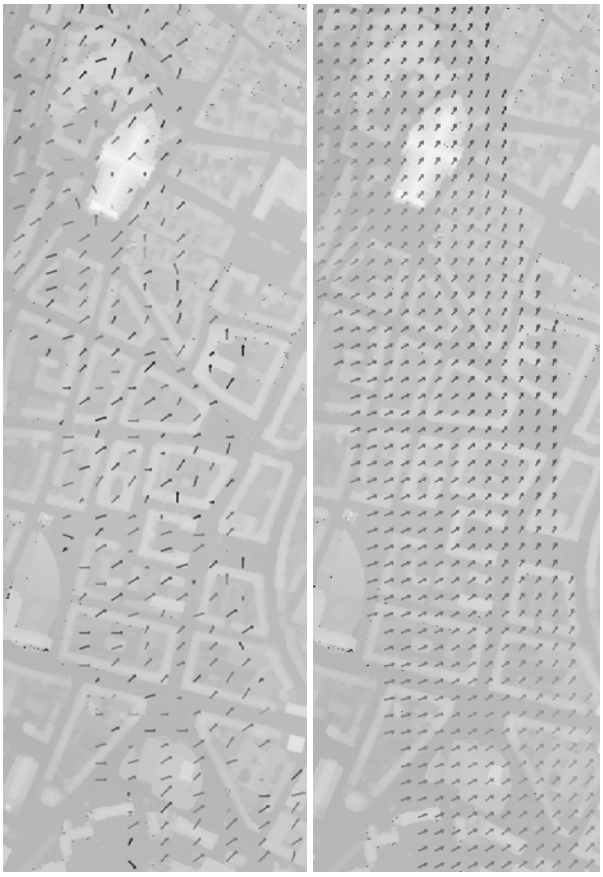

(a) Local measurements (b) Sliding window model using affinities

Figure 5: Measured and modeled deformation field for registering a laser strip with regard to a photogrammetric DSM.

5 Conclusion

The problem of combining data acquired from different sensors enlights at first the non coherence of mutual geometries. It is particularly the case when using together lidar data and photogrammetric data since i) they can have been acquired at two different times, and ii) the georeferencing process of both technologies is far apart if bundle block adjustement is used for photogrammetry. We have presented in this paper a full methodology for registering a couple of topographic surfaces acquired from different sensors. If the first part of the algorithm concerning surface local matching may be considered as a generic tool, the second part consists in deriving a continuous tridimensionnal deformation field designed for registering an airborne laser strip with regard to a photogrammetric DSM.

The future work consists in using the geometrical coherence of lidar and photogrammetric data for working on the effective fusion of both technologies.

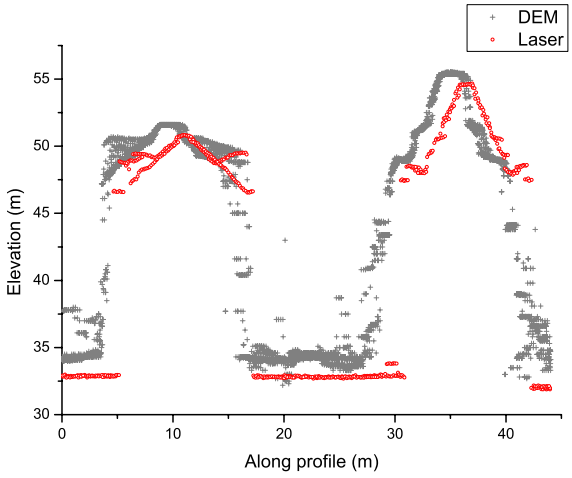

(a) Before registration

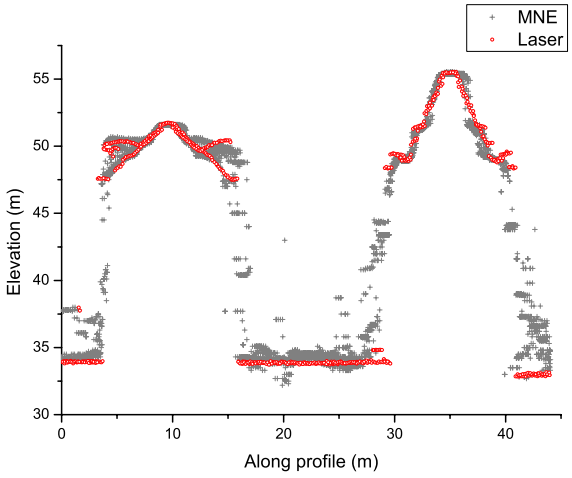

(b) After registration

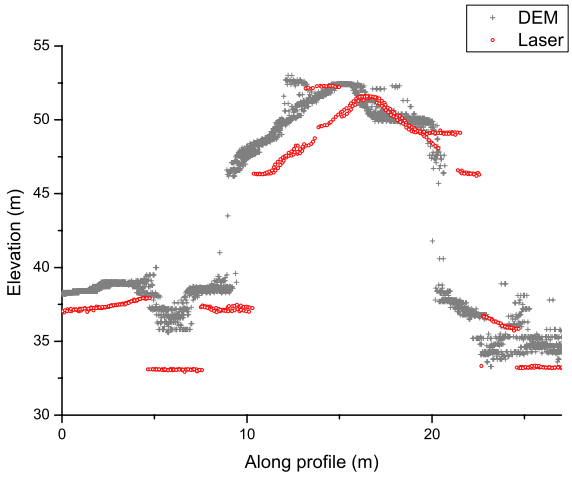

(c) Before registration

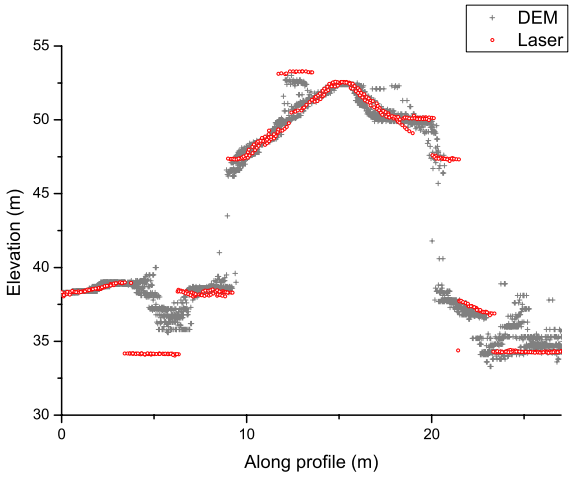

(d) After registration

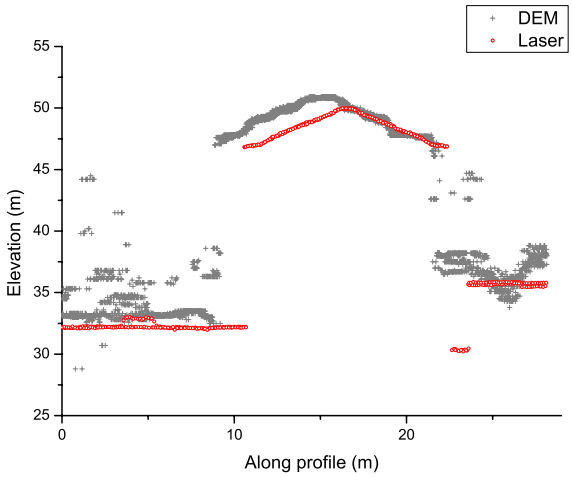

(e) Before registration

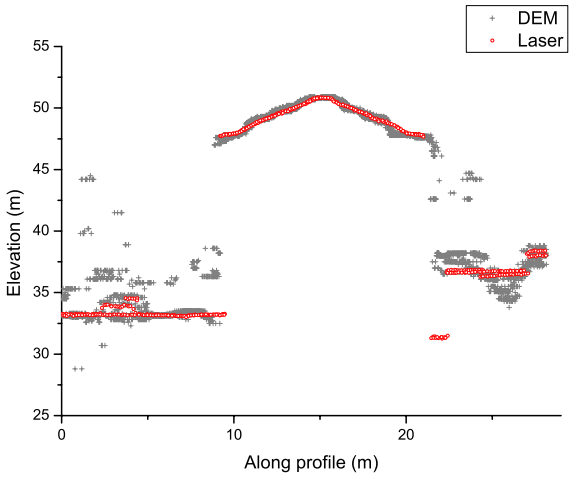

(f) After registration

Figure 6: Profiles of both DSM points (gray crosses) and laser points (red circles) **before** and **after** the registration process over building structures.

REFERENCES

Baillard, C. and Dissard, O., 2000. A stereo matching algorithm for urban digital elevation models. Photogrammetric Engineering and Remote Sensing.

Habib, A., Ghanma, M., Morgan, M. and Al-Ruzouq, R., 2005. Photogrammetric and Lidar Data Registration Using Linear Features. Photogrammetric Engineering & Remote Sensing 71(6), pp. 699–707.

Kager, H., 2004. Discrepancies between overlapping laser scanner strips - Simultaneous fitting of aerial laser scanner strips. Vol. XXXV, XXth ISPRS Symposium - International Archives of Photogrammetry and Remote Sensing, Istanbul, Turkey.

Katzenbeisser, R., 2003. About the Calibration of Lidar Sensors. Vol. XXXIV, Proceedings of the ISPRS Workshop III/3 "3D Reconstruction from Airborne Laserscanner and InSAR" - International Archives of Photogrammetry and Remote Sensing, Dresden, Germany, pp. 59–64.

Kilian, J., Haala, N. and Englich, M., 1996. Capture and evaluation of airborne laser scanner data. Vol. XXXI, International Archives of Photogrammetry and Remote Sensing, pp. 383–388, Part B3.

Ronnholm, P., 2004. The evaluation of the internal quality of laser scanning strips using the interactive orientation method and point clouds. Vol. XXXV-3/W3 part B, XXth ISPRS Symposium - International Archives of Photogrammetry and Remote Sensing, Istanbul, Turkey.

Schenk, T., 2001. Modeling and analysing systematic errors in airborne laser scanners. Technical report, Departement of Civil and Environmental Engineering and Geodetic Science.

Xu, G. and Zhang, Z., 1996. Epipolar Geometry in stereo, motion and object recognition. Kluwer Academic Publishers.